

Development of a Supersonic Flow Chemical CO Laser Driven by a Chemical Reaction between Carbon Vapor and Oxygen

E. Jans, K. Frederickson, M. Yurkovich, Z. Eckert, J.W. Rich, and I.V. Adamovich

Department of Mechanical and Aerospace Engineering

The Ohio State University, Columbus, OH 43210

Abstract

A chemical flow reactor is used to study the vibrational population distribution of CO produced by a reaction between carbon vapor generated in an arc discharge and molecular oxygen. The results demonstrate formation of highly vibrationally excited CO, up to vibrational level $v=14$, at low temperatures, $T=400-450$ K, with population inversions at $v=4-7$, in a collision-dominated environment, 15-20 Torr. The average vibrational energy per CO molecule formed by the reaction is 0.6-1.2 eV/molecule, which corresponds to 10-20% of the reaction enthalpy. The results show feasibility of development of a new CO chemical laser using carbon vapor and oxygen as reactants.

A supersonic flow CO laser excited by a transverse RF discharge in the plenum is used to determine the effect of adding air species to the laser mixture. Carbon monoxide infrared emission spectra are used to measure CO vibrational level populations and temperature in subsonic CO-He, CO-He-N₂, CO-He-O₂, and CO-He-air flows excited by the discharge. Laser power and spectra generated in the transverse resonator in the $M=3$ supersonic flow are measured for each mixture. Nitrogen addition to the baseline CO-He mixture increases energy stored in the CO vibrational mode, resulting in a significant increase in laser power. Addition of oxygen had the opposite effect, reducing both CO vibrational populations and laser power. Adding air resulted in a modest increase of CO vibrational distribution, as well as an increase in laser power, although not as significant as when nitrogen was added to the flow. The experimental results are compared with kinetic modeling predictions, showing good agreement. The results demonstrate feasibility of operating a supersonic flow CO laser in mixtures with significant amounts of air.

1. Generation of Vibrationally Excited CO in a Chemical Reaction between Carbon Vapor and Oxygen

Exothermic chemical reactions are commonly used for extraction of energy, where reactants are chemically converted to lower energy products and the excess chemical energy is converted to work. Chemical lasers utilize these types of chemical reactions, where chemical energy is stored in internal modes of the products and is then extracted through the stimulated emission process producing laser power. Recent theoretical and experimental studies of the exothermic reaction of atomic carbon and molecular oxygen have suggested that a significant fraction of the excess chemical energy (up to $\sim 30\%$) is stored in the vibrational mode of the carbon monoxide product. These results suggest a potential development of a chemical carbon monoxide laser based on this reaction.

Electric discharge excited CO lasers, first demonstrated by Patel [1] and Osgood and Eppers [2], emit in the mid-infrared spectral band and have been reported to operate with efficiencies as large as 50% [3] and powers up to 200 kW [4]. The reported optimal performance was achieved using electric discharges operated at cryogenic temperatures. In these systems, laser gain is established on ro-vibrational transitions within the ground electronic state of the CO molecule by rapid vibration-to-vibration (V-V) quanta exchange among molecules in vibrationally excited levels initially populated by electron impact in the discharge. This V-V exchange process was first described by Treanor *et al* [5] who explained the kinetics which result in a highly non-Boltzmann vibrational distribution among vibrational levels of molecules in low-temperature environments. It was shown by Rich [6] to cause the partial population inversions between ro-vibrational levels and laser gain along P-branch lines in a high power CO laser.

Current versions of chemical carbon monoxide lasers, specifically, those based on the reaction of carbon disulfide and molecular oxygen, present similar characteristics to the electric discharge type, i.e., they both show laser gain on the higher, more anharmonic, vibrational band components. The dominant CO product of $\text{CS}_2 + \text{O}$ and $\text{CS} + \text{O}$ reactions contains several vibrational quanta [7], with peak population in $v=12$ [8]. Carbon disulfide, however, is a highly toxic compound and more costly than the common allotropes of carbon, such as graphite, making it a less desirable precursor. A novel chemical carbon monoxide laser based on the gas-phase reaction between atomic carbon vapor and molecular oxygen would exhibit numerous advantages over the current chemical or electric discharge carbon monoxide lasers. High power and efficiency would be achievable due to the relatively slow vibration-to-translation (V-T) and vibration-to-rotation (V-R) quanta loss, which is a characteristic property of carbon monoxide, and higher gain associated with the total population inversions found in chemical lasers could also be achieved. Finally, complications of using carbon disulfide would be removed by implementing the use of graphite or amorphous carbon as the carbon source in the reaction.

Molecular dynamics simulations have predicted one of the dominant products of this reaction would be vibrationally excited CO in the ground electronic state. The heat of reaction



$\Delta H = -132.6$ kcal/mol (5.75 eV), is sufficiently large to populate a number of excited vibrational levels (CO vibrational quantum is approximately 0.26 eV). Subsequent crossed molecular beam experiments confirmed that the CO product is vibrationally excited. These results also demonstrate total population inversions over the first five vibrational levels. Higher vibrational

levels could not be observed due to spectral bandwidth limitations of the laser probe. The first objective of the present work is to detect vibrationally excited CO product of a chemical reaction between carbon sublimation products and oxygen, at pressures and temperatures suitable for development of a chemical CO laser.

The oxidation of carbon vapor generated in an arc discharge in argon buffer was studied in a custom-made flowing chemical reactor, shown schematically in Fig. 1. The reactor consists of a six-arm cross stainless steel cell and a 1" diameter glass observation cell, the first cell housing a DC arc discharge electrode assembly, and the other used for *in situ* spectroscopic diagnostics. The arc discharge cell arms are 2" in diameter, two opposing arms are used to provide access for the arc discharge electrode mounts. The powered electrode is a tungsten rod 1/4" in diameter, and the grounded electrode is a graphite carbon rod 2 mm in diameter, attached to vacuum-sealed electrode mounts. During the operation, the gap between the electrodes is adjusted by a computer controlled stepper motor (Haydon Kerk 43HGJ-05-A01), coupled to the translatable grounded electrode mount. Two other arms are used for inlet argon buffer gas flow through a 1/2" diameter quartz tube extending into the arc discharge cell, and for exit of carbon electrode sublimation products, through a 2.5" to 1" diameter glass adapter 5 cm long connected to the observation cell, as shown in Fig. 1. The distance between the buffer gas inlet flow tube and the arc discharge electrodes is approximately 1 cm. The buffer flow entrains the carbon vapor products to minimize their accumulation in the arc discharge cell. The pressure in the cell is 15-20 Torr, and the argon buffer flow rate is varied in the range of 2-12 slm.

The electrodes are powered by a 100 V, 150 A DC power supply. The arc discharge is initiated by advancing the grounded electrode toward the powered electrode until they were brought in contact with each other, after which the grounded electrode is retreated by ~1-2 mm while the discharge is maintained. In the present work, the discharge is operated at 20 V and 35 A, for a duration of 60 s. During operation, the gap between the electrodes increases, by up to ~1-2 mm, due to carbon sublimation of the grounded electrode. However, this moderate increase of the electrode gap did not terminate the discharge, such that advancing of the grounded electrode during the operation was not necessary. The vapor-phase carbon products generated by the arc discharge is entrained into the Ar buffer flow and is transferred to the observation cell, which is 40 cm long, with CaF₂ windows attached to the flanges at both ends (see Fig. 1). This provides optical access for *in situ* infrared absorption and emission measurements.

A flow of oxygen or a 20% O₂/Ar mixture is injected into the observation cell tube in the direction opposite to that of the carbon vapor – argon buffer flow, as shown in Fig. 1, at a flow rate of ~100 sccm. The reaction products formed in the counter-flow mixing region traverse the 40 cm length of the observation cell and exit near the opposite end, such that the optical axis is parallel to the gas flow. For absorption measurements, emission from a calibrated blackbody source (InfraRed Industries Inc. Model 563), maintained at a temperature of 1000 °C, was focused into the absorption cell using a pair of off-axis parabolic mirrors, as shown in Fig. 1, and directed into the emission port of a Bruker IFS/66s Fourier Transform Infrared (FTIR) spectrometer by another pair of mirrors, to detect the products of the carbon vapor reaction with oxygen. The optical path length for these measurements is 40 cm. The same signal collection was used for infrared emission measurements from the observation cell, to detect vibrationally excited states of the reaction products. For emission measurements, the blackbody source was blocked, and the FTIR was focused approximately in the center of the observation cell, 15 cm from injection of carbon vapor / argon and oxygen flows. In the present experiments, the FTIR

was operated at spectral resolution of 0.25 cm^{-1} , averaging 100 scans during the 60 s arc discharge operation time.

Figure 2 shows a sample FTIR fundamental emission spectrum from the observation cell, taken during the carbon arc discharge operation and counterflow injection of oxygen into the observation cell, as shown in Fig. 1. The pressure and flow rate of argon buffer are $P_{\text{Ar}}=17.6\text{ Torr}$ and 5 slm , respectively, and oxygen partial pressure is $P_{\text{O}_2}=0.05\text{ Torr}$. At these conditions, the carbon monoxide partial pressure in the observation cell, estimated using calibration CO absorption spectra taken at different CO pressures, is several mTorr. The spectrum is taken at 0.25 cm^{-1} resolution, such that rotational structure of CO fundamental emission bands is resolved. Detected CO fundamental emission bands extend from 2240 cm^{-1} to the FTIR InSb detector cutoff near 1850 cm^{-1} . No CO_2 bands were detected in the emission or absorption spectra. Figure 2 also compares the experimental CO fundamental emission spectrum with a best fit synthetic spectrum. The synthetic spectrum was calculated at the same spectral resolution, taking into account accurate rotational-vibrational line positions, intensities, and Einstein coefficients for spontaneous emission, and the FTIR spectrometer response function measured using the calibrated blackbody source, as was done in our previous work [9]. The synthetic spectra are used for inference of CO vibrational level populations.

Figure 3 shows a Boltzmann plot of R-branch transitions of the $\text{CO}(v=1\rightarrow 0)$ emission band for the experimental spectrum in Fig. 3, indicating a rotational-translational temperature of $T=400\pm 10\text{ K}$. Deviation from the straight line at $J\leq 8$ in Fig. 3 is caused by the overlap between CO rotational lines in $1\rightarrow 0$ and $2\rightarrow 1$ bands. This demonstrates that in spite of high temperature in the carbon arc discharge, the temperature in the observation cell, where CO is formed by a chemical reaction, is quite low. At these conditions, the estimated flow velocity through the observation cell is approximately 10 m/s . The flow in the observation cell remains optically thin, such that self-absorption on CO fundamental transitions remains a minor factor and does not affect the accuracy of temperature or vibrational population inference. Fig. 4 plots CO vibrational level relative populations inferred from synthetic fundamental emission spectra such as shown in Fig. 2, for two different flow rates, 5 slm and 12 slm . Translational-rotational temperatures are indicated in the plots.

From Fig. 4, it can be seen that increasing the argon buffer flow rate through the reactor from 5 slm to 12 slm , while keeping the pressure approximately the same, $P=17\text{-}19\text{ torr}$, results in significant increase of high CO vibrational level populations, up to a factor of two at $v=8$. At 12 slm , absolute population inversions at $v=4\text{-}7$ are readily apparent. This trend is expected, since increasing the flow rate (i.e. the flow velocity through the observation cell) reduces the reaction product flow residence time from the mixing point to the FTIR mirror focal point, from $\tau_{\text{res}}\sim 15\text{ ms}$ at 5 slm (flow velocity of $\sim 10\text{ m/s}$) to $\tau_{\text{res}}\sim 6\text{ ms}$ at 12 slm (flow velocity of $\sim 24\text{ m/s}$). Comparing this with spontaneous radiative decay of vibrationally excited CO molecules ($\tau_{\text{rad}}\sim 3\text{ ms}$ for $v=10\rightarrow 9$ fundamental transition) suggests that operation at even higher buffer flow rates may be beneficial, as long as the flow residence time exceeds the mixing / chemical reaction time. The room temperature rate of reaction (1) is $k=1.6\cdot 10^{-11}\text{ cm}^3/\text{s}$ [10], which at the present conditions yields $\tau_{\text{chem}}\sim 1/k[\text{O}_2]\sim 10\text{ }\mu\text{s}$ (assuming that $[\text{O}_2]\sim [\text{C}]$), such that the reaction in the observation cell is likely to be mixing limited.

From the results shown in Fig. 4, the average vibrational energy per CO molecule formed by the chemical reaction between carbon sublimation products and oxygen is approximately 0.6 eV/molecule at 5 slm and 1.2 eV/molecule at 12 slm . This represents 10% and 20% of the heat of

reaction (1), respectively. The present measurements likely represent the lower bound value of the heat of reaction fraction stored in the nascent CO vibrational distribution, since the estimated flow residence time exceeds spontaneous radiative decay time of high CO vibrational levels. Further measurements taken at higher buffer flow rate are necessary to produce a more accurate value.

The present results, demonstrating formation of highly vibrationally excited CO, up to at least $v=14$, with absolute population inversions at $v=4-7$, in collision-dominated environments ($P=15-20$ Torr) and at low rotational-translational temperatures ($T=400-450$ K), indicate feasibility of development of a new CO chemical laser using carbon vapor and oxygen as reactants. A high fraction of reaction enthalpy stored in the CO vibrational mode (at least 10-20%) inferred from the present data suggests that this laser may operate at high efficiency. In particular, our previous work, which demonstrated lasing in optically pumped CO-Ar mixtures at $T\approx 300-400$ K and $P=10$ Torr, at CO partial pressures of $\sim 0.2-0.3$ Torr [11] suggests that vibrational excitation of CO in a chemical reaction between carbon and oxygen may be used for laser power generation at the present operating conditions. Further work will focus on enhancing the amount of highly vibrationally excited carbon monoxide produced in the reactor, and detecting small signal gain and lasing.

2. Electrically Excited, Supersonic Flow CO Laser Operated with Air Species in the Laser Mixture

One of the applications of a new chemical CO laser discussed in Section 1 is electrical power generation on board of a hypersonic vehicle. At these conditions, carbon vapor can be generated by carbon surface ablation by a high-speed flow, and subsequently mixed with air to produce vibrationally excited CO in a chemical reaction with oxygen, as discussed in Section 1. Laser power would be generated in a supersonic flow laser cavity and converted to electrical power using photovoltaic cells. Thus, the laser would have to operate in a gas mixture with a significant fraction of air. Additionally, the flow temperature in the laser cavity may be high, due to an oblique shock system slowing the flow upstream of the cavity. However, lasing at elevated temperatures has been demonstrated. Optically pumped CO laser operation in a CO-Ar mixture, at temperatures up to $T=450$ K, was demonstrated by Ivanov et al [11] and chemical CO laser operation in a $CS_2-O_2-He-Ar$ mixture was demonstrated at temperatures up to $T=500\pm 200$ K by Boedeker et al [12]. Adding nitrogen and oxygen to the laser mixture may significantly affect CO vibrational distribution function, both due to vibration-vibration (V-V) energy transfer to N_2 and O_2 and due to vibration-translation (V-T) relaxation by O atoms.

Previous measurements of vibrational populations of CO, N_2 , and O_2 in optically pumped CO- N_2 , CO- O_2 , and CO-air mixtures by Lee et al [13] demonstrated the effect of air species on the vibrational energy distribution of CO. In these experiments, low vibrational states of CO were excited by resonance absorption of CO pump laser radiation, followed by V-V energy exchange among CO, N_2 , and O_2 molecules. The results show that presence of nitrogen has a weak effect on the CO vibrational distribution function, due to the fact that nitrogen has larger energy spacing between vibrational levels, compared to that of CO, such that the rate of V-V energy transfer from CO to N_2 is lower compared to the rate of the reverse process. Because of this, most of the vibrational energy available in the mixture remains in the CO vibrational mode,

with relatively little vibrational excitation of N_2 [13]. Adding oxygen to the mixture, on the other hand, considerably reduces energy stored in the CO vibrational mode, such that O_2 vibrational populations exceed those of CO [13]. This occurs since O_2 has a smaller vibrational energy spacing compared to that of CO, such that vibrational energy is preferentially transferred from CO to O_2 by V-V exchange processes. These results demonstrate the negative impact that oxygen has on vibrational excitation of CO, which is critical for laser operation.

The second objective of the present work is to study how adding significant amounts of nitrogen, oxygen, or air to the laser mixture affects CO laser power and spectrum. For this, we use an electric discharge excited, supersonic flow CO laser. Supersonic expansion is used to reduce the temperature of the laser mixture and to study laser operation in a high speed flow, such as would occur in a hypersonic flight.

The supersonic flow laser apparatus used in the present investigation, shown schematically in Fig. 5, is similar to the electric discharge excited oxygen iodine laser developed in our previous work [14]. Briefly, gas mixture components (carbon monoxide, helium, oxygen, nitrogen, and air) are delivered from high-pressure cylinders and premixed in a 1 inch diameter, 5 m long delivery line, before flowing through a 10 cm x 2 cm rectangular cross section, 10 cm long electric discharge section, which serves as a plenum of a supersonic flow channel made of acrylic plastic (see Fig. 5). Individual flows are activated by remotely controlled solenoid valves. Two electrode blocks are flush mounted in the top and bottom walls of the discharge section. Each electrode is a 10 x 10 cm copper plate, covered by an alumina ceramic plate 1.6 mm thick, which prevents secondary electron emission from the electrode surface and improves discharge stability. The electrodes are powered by a Dressler 5 kW, 13.56 MHz RF power supply with automatic impedance matching network.

Downstream of the discharge section, the flow enters an optical access section, 7.6 cm long, equipped with CaF_2 windows flush mounted in the top and side walls. This section was in place only for CO infrared emission spectra measurements and was removed during laser spectra and power measurements to shorten the distance between the discharge section and the supersonic nozzle. The emission spectra are measured by a Varian 660-IR Fourier Transform Infrared (FTIR) spectrometer. The 7 cm long nozzle, with 0.32 cm x 10 cm throat cross sectional area, has an expansion ratio designed for an exit Mach number of $M=3$. Downstream of the nozzle exit, the flow enters the supersonic section with entrance height of 1 cm. The top and bottom walls of the supersonic channel diverge at 1.5° angle each, to allow for boundary layer growth. Several 0.5 inch diameter apertures in the side walls of the supersonic section, made of aluminum, provide optical access to the flow, as shown in Fig. 5. Two optical mounts with 1 inch diameter, 1 m radius of curvature laser mirrors, with 99.8% reflectivity between 4.5 and $5.75 \mu m$ (Rocky Mountain Instruments) are attached to the walls 3.2 cm downstream of the nozzle exit, forming a transverse laser cavity, with laser power coupled out on both sides of the cavity. During the experiments, laser spectra and laser power are measured simultaneously. Laser power is measured using the beam on one side of the resonator, by a Scientech AC5000 power meter, and multiplied by two. Laser spectrum is measured using the beam on the other side of the resonator, by the Varian FTIR spectrometer. Downstream of the supersonic section, the flow enters a 36 cm long diffuser with top and bottom walls diverging at 3° , before exhausting into a 750 ft^3 vacuum tank pumped down by a 300 cfm vacuum pump. The steady state supersonic flow run time is approximately 5 s.

Figure 6 plots the CO infrared overtone emission spectra measured downstream of the discharge section in two different mixtures with the same amount of carbon monoxide and helium, 3.6 Torr CO - 97 Torr He and 3.6 Torr CO - 97 Torr He - 13.8 Torr N₂, at the same RF discharge power of 2 kW. These spectra, shown on the same scale, are used to infer CO vibrational level populations, as discussed in Section 1. Fundamental spectra, taken at the same conditions are used for rotational temperature inference. It is evident that adding nitrogen to the mixture results in considerable increase in emission intensity over a wide range of CO overtone transitions.

The kinetic model used to predict CO vibrational level populations and laser spectra in the supersonic cavity incorporates state-to-state vibrational kinetics, including vibration-vibration (V-V) energy transfer processes among CO, N₂, and O₂ and vibration-translation (V-T) relaxation of diatomic species by CO, N₂, O₂, Ar, He, and O atoms [13,15,16]; chemical kinetics equations for species number densities in a reacting mixture; and quasi-one-dimensional compressible flow equations of vibrationally nonequilibrium, reacting flow. Since direct measurements of the electric field in the positive column of transverse RF discharge are challenging, the reduced electric field (E/N) in the discharge is considered an adjustable parameter, determined from matching the predicted CO vibrational distribution function (VDF) to the experimental VDF inferred from CO infrared emission spectra measured downstream of the discharge section. Rate coefficients of vibrational excitation of CO, N₂, and O₂ by electron impact, as well as rate of O₂ dissociation by electron impact are calculated by solving Boltzmann equation for plasma electrons [17]. The model also includes a set of laser field equations governing the stimulated emission intensity on each lasing vibrational transition in transverse laser cavity [18]. On each vibrational band, lasing is assumed to occur on a single vibrational-rotational transition with maximum gain. To simulate lasing at steady-state conditions, the intracavity photon flux on each vibrational band is assumed to be constant throughout the cavity, chosen such that the laser power on that band matches the cavity-averaged power loss from the CO vibrational mode due to stimulated emission. Input parameters of the model are the gas mixture composition, RF discharge power, supersonic nozzle geometry, cavity gain length, cavity mirror reflectivities, and clear aperture mirror surface area.

Figure 7 plots temperature downstream of the discharge, inferred from the rotational structure of CO fundamental emission band, as discussed in Section 1, showing that the temperature is in the range T=380-425 K. Figure 8 plots experimental CO vibrational distribution functions inferred from emission spectra such as plotted in Fig. 6, compared with the modeling predictions. As discussed above, in the modeling calculations the reduced electric field value, E/N, was adjusted to obtain the best match between the experimental and predicted CO VDFs. It can be seen that in both in the baseline CO-He mixture and in mixtures containing N₂, O₂, and air, experimental and the predicted CO vibrational populations are fairly close to each other, indicating that the rates of V-V exchange for CO-CO, CO-N₂, and CO-O₂, which control the CO VDF at these conditions are represented fairly accurately.

Figure 9 compares laser spectra taken at the same RF discharge power of 2 kW in CO-He-N₂ and CO-He-air mixtures. It can be seen that in CO-He-N₂ mixture, lasing occurs on fundamental vibrational bands ranging from $v=2 \rightarrow 1$ to $v=15 \rightarrow 14$, on several rotational transitions in each band. The laser spectrum exhibits evidence of laser cascade, when lasing on higher vibrational transitions overpopulates lower vibrational levels and triggers lasing on lower transitions. Lasing on relatively low rotational transitions, $J'=6-14$, is typical for low

translational-rotational temperature in the laser cavity, estimated to be $T \approx 130$ K from CO fundamental infrared emission spectra taken from the supersonic flow and predicted to be $T = 110$ K. Replacing nitrogen with air produces a similar spectrum, except that lasing occurs on vibrational bands ranging from $v=3 \rightarrow 2$ to $v=13 \rightarrow 12$, on fewer rotational transitions. It can be seen that the modeling predictions reproduce the range of vibrational transitions on which lasing occurs (except for the lowest vibrational transition in CO-He-N₂), as well as the rotational quantum numbers on which the laser power in each vibrational band peaks fairly well. Note that, as discussed above, the present model assumes that lasing occurs only on one vibrational-rotational transition in each band, on which gain reaches maximum.

Figure 10 illustrates the effect of adding N₂, O₂, and air to the baseline CO-He mixture on laser output power, at constant CO partial pressure of 3.6 Torr and RF discharge power of 2 kW. The data show that adding nitrogen to the laser mixture results in a dramatic increase of laser power, from 8-10 W to approximately 30 W, at N₂ partial pressures of 10-30 Torr. This trend is consistent with CO vibrational population increase in the presence of nitrogen (see Fig. 8(a,b)), and may also be affected by translational-rotational temperature reduction as N₂ partial pressure is increased, from $T = 393 \pm 6$ K in the baseline CO-He mixture to $T = 361 \pm 5$ K in the mixture with 20.3 Torr of nitrogen (see Fig. 7). The temperature reduction is likely caused by the increase in the fraction of discharge input energy going to vibrational excitation of nitrogen, thereby reducing energy fraction to electronic excitation of helium, which contributes to a temperature rise during collisional quenching.

Adding oxygen to the baseline CO-He laser mixture dramatically reduces the laser power, by over an order of magnitude with less than 7 Torr of O₂ added (see Fig. 10). Again, this is consistent with CO vibrational population reduction in the presence of oxygen (see Fig. 8(c)) and modest temperature rise as O₂ partial pressure is increased, from $T = 393 \pm 6$ K in the baseline CO-He mixture to $T = 410 \pm 6$ K in the mixture with 8.7 Torr of oxygen (see Fig. 7). Finally, adding air to the baseline mixture results in the laser power increase, by almost a factor of two (see Fig. 10), such that the effect of nitrogen appears to outweigh that of oxygen, qualitatively consistent with modest CO vibrational population increase (see Fig. 8(d)) and slight temperature reduction as air partial pressure is increased, from $T = 393 \pm 6$ K in the baseline mixture to $T = 384 \pm 9$ K in the mixture with 21.3 Torr of air (see Fig. 7). The highest laser output power is measured in a 3.3 Torr CO, 97 Torr He, 13.4 Torr N₂ mixture excited by a 2000 W RF discharge, producing 32.4 W, at an efficiency of 1.6%.

The kinetic modeling predictions reproduce the trend for the laser power increase as nitrogen is added to the baseline CO-He mixture, although the absolute laser power is overpredicted by approximately a factor of 2 (see Fig. 10). This is most likely caused by neglecting the cavity losses other than transmission through the laser mirrors. The model also overpredicts the rate of laser power reduction as significant amount of air (up to 30%) is added to the baseline CO-He mixture (see Fig. 10). Analysis of the results suggests that this occurs due to overprediction state-specific rates of V-T relaxation of high vibrational levels of CO by O atoms. These rates have not been measured experimentally, and are based on extrapolation of the experimental results for vibrational relaxation time [19], using a simple collinear collision theory [20].

The present results demonstrate that significant CO vibrational nonequilibrium and lasing can be obtained in vibrationally excited CO-air flows, with significant mole fraction of air (up to at least 20-30%). Higher mole fractions of air in the flow have not been tested because sustaining

a stable and diffuse RF discharge at these conditions would be challenging. The results of the present work suggest that, given a sufficiently strong CO vibrational excitation source, produced by electric discharge, optical pumping by another CO laser, or by nonequilibrium chemical reaction at moderate stagnation temperatures (300-400 K), continuous wave lasing can be produced in CO-air mixtures after supersonic expansion to $M=3$.

3. Acknowledgments

The authors acknowledge the support of Lockheed Martin Corporation and project technical monitor Dr. Luke Uribarri. We also wish to acknowledge the support of the Michael A. Chaszeyka gift. Finally, we are grateful to Prof. George Shatz from Northwestern University and Prof. Tim Minton from Montana State University for sharing with us the results of molecular dynamics modeling and molecular beam studies of the $C + O_2$ reaction.

References

1. Patel, C.K.N., "Vibrational-Rotational Laser Action in Carbon Monoxide", *Phys. Rev.* 141, 71, 1966
2. Osgood, R.M. Jr., and Eppers, E.R., "High-Power CO-N₂-He Laser", *Appl. Phys. Lett.* 13, 409, 1968
3. Grigor'yan, G.M., Dymshits, B.M., and Izyumov, S.V., *Sov. J. Quant. Electron.* 17, 1385, 1987
4. Dymshitz, B.M., et al., "CW 200 kW Supersonic CO Laser", *Proc. SPIE* 2206, 109, 1994
5. Treanor, C.E., Rich, J.W., and Rehm, R.G., "Vibrational Relaxation of Anharmonic Oscillators with Exchange-Dominated Collisions", *J. Chem. Phys.* 48, 1798, 1968
6. Rich, J.W., "Kinetic Modeling of the High-Power Carbon Monoxide Laser", *J. Appl. Phys.* 42, 2719, 1971
7. Dudkin, V.A., "Chemical CO Lasers Based On Carbon-Disulfide Flame", *Journal of Russian Laser Research* 20, 362, 1999
8. M. C. Lin, M. E. Umstead, and N. Djeu, "Chemical Lasers", *Annual Review of Physical Chemistry* 34, 557, 1983
9. E. Ploenjes, P. Palm, A.P. Chernukho, I.V. Adamovich, and J.W. Rich, "Time-Resolved Fourier Transform Infrared Spectroscopy of Optically Pumped Carbon Monoxide", *Chem. Phys.* 256, 315, 2000
10. G. Dorthe, Ph. Caubet, Th. Vias, B. Barrere, and J. Marchais, "Fast flow studies of atomic carbon kinetics at room temperature", *J. Phys. Chem.* 95, 5109, 1991
11. Ivanov, E., Frederickson, K., Leonov, S., Lempert, W.R., Adamovich, I.V., and Rich, J.W. "Optically Pumped Carbon Monoxide Laser Operating at Elevated Temperatures", *Laser Physics* 23, 095004, 2013

12. Boedeker, L. R., Shirley, J. A., & Bronfin, B. R., "Arc-excited flowing CO chemical laser", *Applied Physics Letters*, 21, 247-249, 1972
13. W. Lee, I.V. Adamovich, and W.R. Lempert, "Optical Pumping Studies of Vibrational Energy Transfer in High-Pressure Diatomic Gases", *J. Chem. Phys.* 114, 1178, 2001
14. J.R. Bruzzese, A. Hicks, A. Erofeev, A.C. Cole, M. Nishihara, and I.V. Adamovich, "Gain and Output Power Measurements in an Electrically Excited Oxygen-Iodine Laser with a Scaled Discharge", *J. Phys. D: Appl. Phys.* 43, 015201, 2010
15. E. Ploenjes, P. Palm, A.P. Chernukho, I.V. Adamovich, and J.W. Rich, "Time-Resolved Fourier Transform Infrared Spectroscopy of Optically Pumped Carbon Monoxide", *Chemical Physics*, vol. 256, 2000, pp. 315-331
16. E. Ploenjes, P. Palm, W. Lee, M. D. Chidley, I.V. Adamovich, W.R. Lempert, and J. William Rich, "Vibrational Energy Storage in High-Pressure Mixtures of Diatomic Molecules", *Chemical Physics*, vol. 260, 2000, pp. 353-366
17. G.J.M. Hagelaar and L.C. Pitchford, "Solving the Boltzmann equation to obtain electron transport coefficients and rate coefficients for fluid models", *Plasma Sources Science and Technology* 14 (2005) 722-733; LXcat database, <http://www.lxcat.laplace.univ-tlse.fr>
18. S.D. Rockwood, J.E. Brau, W.A. Proctor, and G.H. Canavan, "Time-Dependent Calculations of Carbon Monoxide Laser Kinetics", *IEEE Journal of Quantum Electronics*, vol. 9, 1973, pp. 120-129
19. Mark E Lewittes, Christopher C Davis, and Ross A McFarlane, "Vibrational deactivation of CO(v=1) by oxygen atoms", *J. Chem. Phys.*, 69(5), 1978
20. Rapp, D., and Kassal, T., "The Theory of Vibrational Energy Transfer between Simple Molecules in Nonreactive Collisions", *Chemical Reviews*, vol. 69, 1969, pp. 61-102

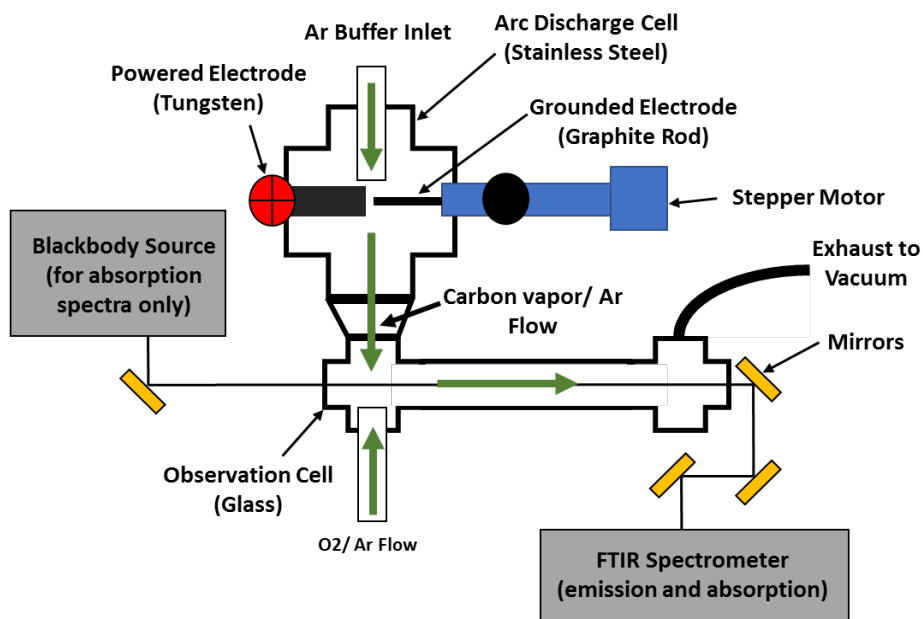


Figure 1. Schematic of the experimental setup for CO generation by a chemical reaction between carbon vapor and oxygen.

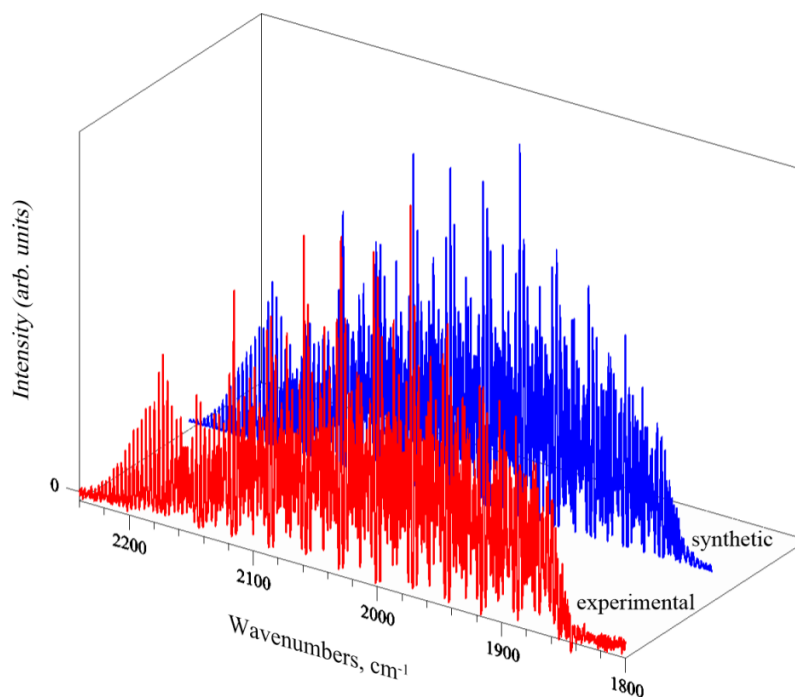


Figure 2. Comparison of experimental and synthetic CO emission spectra in the observation cell. Ar buffer flow pressure 17.2 Torr, O₂ partial pressure 0.05 Torr, flow rate 5 slm.

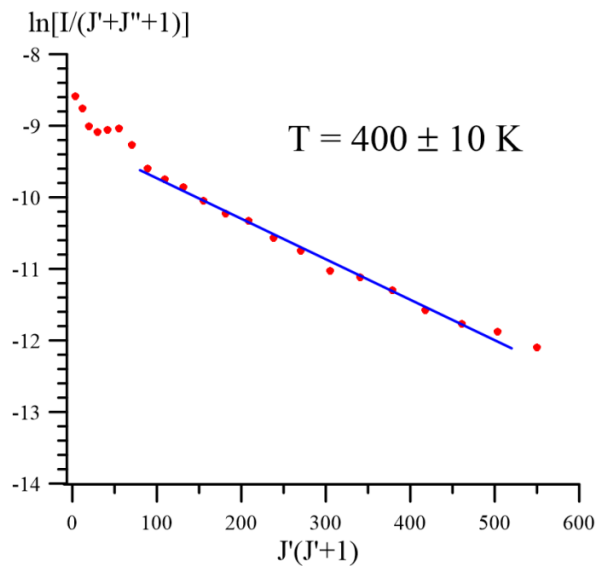


Figure 3. Boltzmann plot of R-branch transitions of CO($v=1 \rightarrow 0$) vibrational band for the experimental spectrum in Fig. 3, indicating rotational temperature of $T=400 \pm 10$ K.

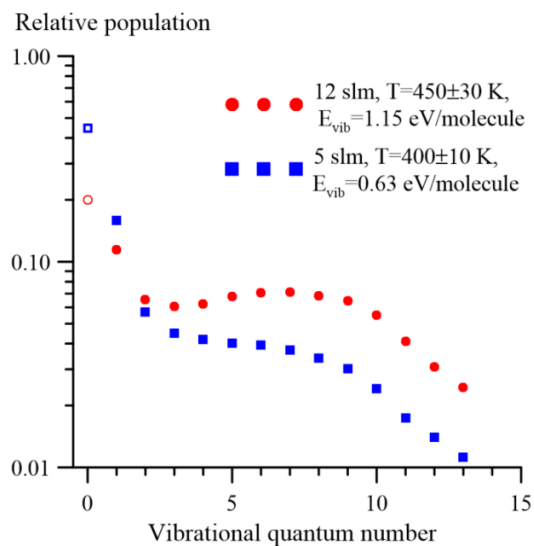


Figure 4. CO vibrational level relative populations inferred from synthetic fundamental emission spectra such as shown in Fig. 3, for two different flow rates. Translational-rotational temperatures and average vibrational energies per CO molecule are indicated in the plots.

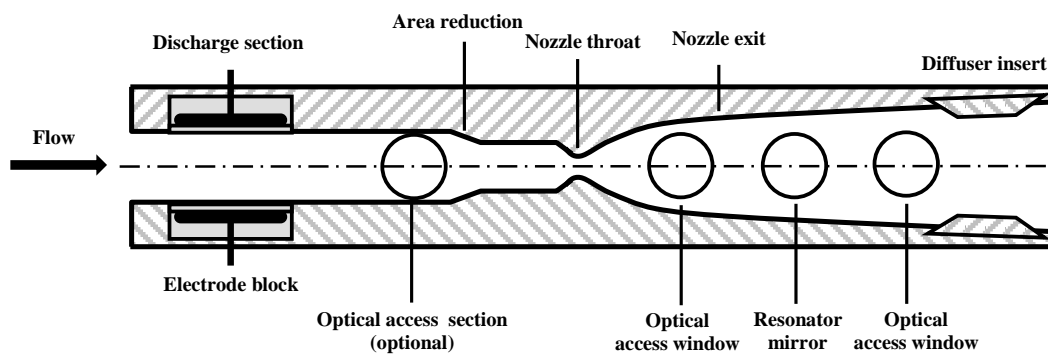


Figure 5. Schematic of the supersonic flow CO laser apparatus.

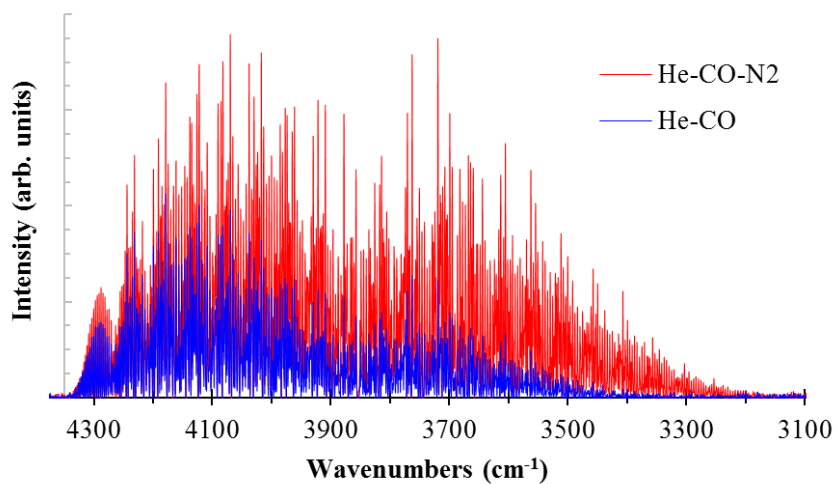


Figure 6. CO infrared emission overtone spectra downstream of the discharge section in 3.6 Torr CO - 97 Torr He and in 3.6 Torr CO - 97 Torr He - 13.8 Torr N₂ mixtures. Resolution 0.25 cm⁻¹, RF discharge power 2 kW.

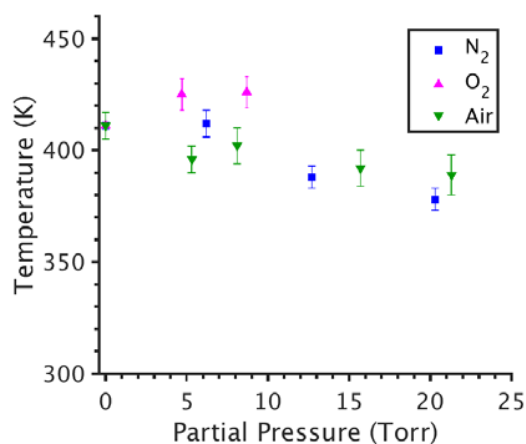


Figure 7. Flow temperature in the plenum, downstream of the discharge section, inferred from CO fundamental emission spectra. In all mixtures, CO partial pressure is 3.6 Torr, He partial pressure is 97 Torr, RF discharge power 2 kW.

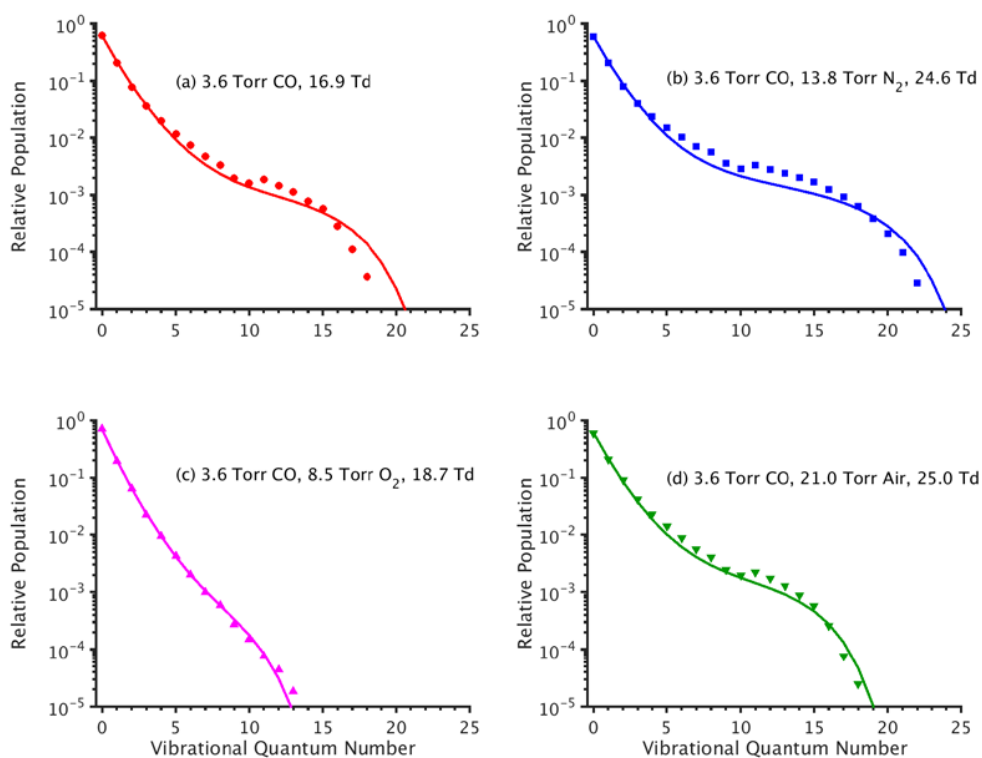


Figure 8. Comparison of CO vibrational distribution functions downstream of the discharge section, with E/N values providing best matching between the data and the modeling predictions: (a) CO-He, (b) CO-N₂-He, (c) CO-O₂-He, and (d) CO-air-He. RF discharge power 2 kW.

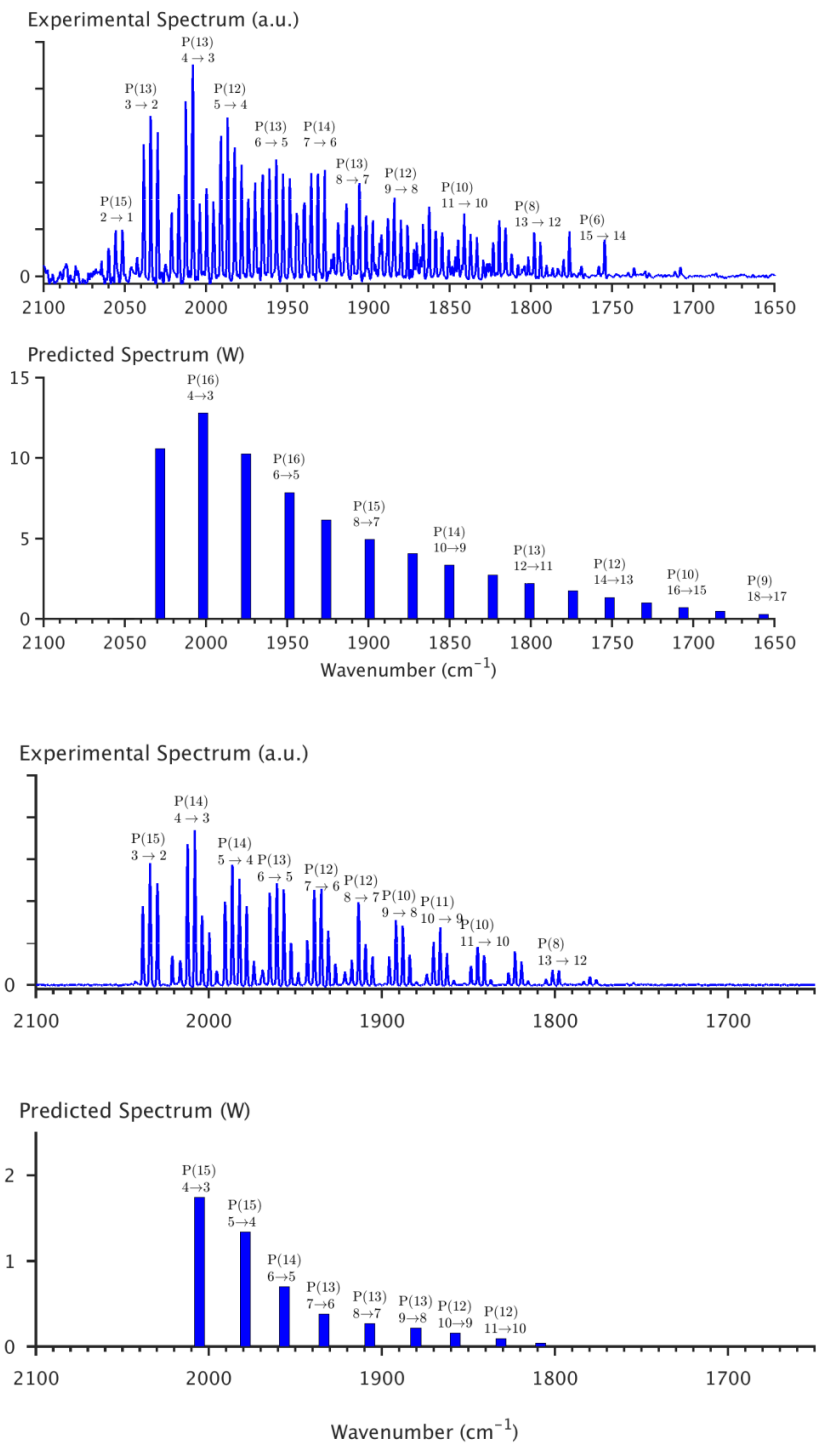


Figure 9. Comparison of experimental and predicted laser spectra in a 3.5 Torr CO - 97 Torr He - 26.3 Torr N_2 mixture (top two figures) and 3.5 Torr CO - 97 Torr He - 32 Torr air mixture (bottom two figures). RF discharge power 2 kW.

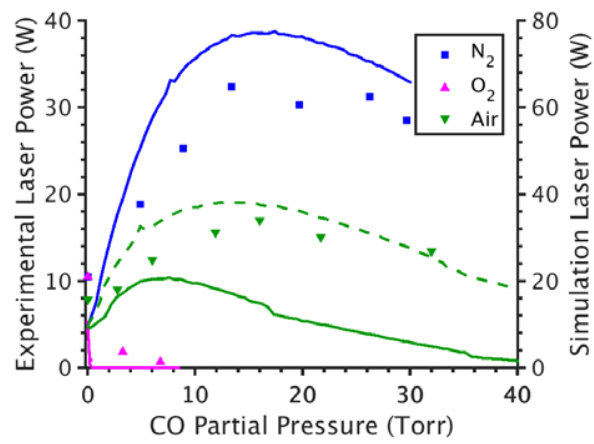


Figure 10. Comparison of experimental and predicted laser power vs. N₂ and air partial pressures in the mixture. CO and He partial pressures 3.6 and 97 Torr, respectively, RF discharge power 2 kW.